Optik 125 (2014) 7227–7230

Contents lists available at ScienceDirect

Optik

journal homepage: www.elsevier.de/ijleo

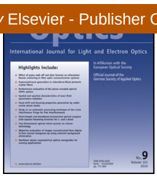

Phase profile analysis of transparent objects through the use of a two windows interferometer based on a one beam splitter configuration

B. Lopez-Ortiz[a], N.-I. Toto-Arellano[a,*], V.H. Flores Muñoz[b], A. Martínez García[b],
L. García Lechuga[a], J.-A. Martínez Domínguez[c]

[a] Centro de Tecnologías Ópticas y Fotónicas de la Universidad Tecnológica de Tulancingo, Hgo. 43642, México
[b] Centro de Investigaciones en Óptica A. C., León, Gto. 37150, México
[c] Ingeniería en Fotónica Área Telecomunicaciones, de la Universidad Tecnológica de Xicotepec de Juárez, Pue. 73080, México

ARTICLE INFO

Article history:
Received 16 December 2013
Accepted 20 July 2014

Keywords:
Two-windows
Phase shifting
Interferometry
Grating
Polarization

ABSTRACT

In this research we implemented a two windows interferometer based on polarization phase shifting and grating interferometry techniques in order to retrieve the phase data profile of the object in a single capture. The optical configuration has two optical beams with circular polarization in opposite directions, and it is coupled with a 4-*f* system. An amplitude grid is used as a filter which is placed at the Fourier plane to obtain replicas of each beam which can properly interfere, depending on the separation between beams. The interferometer presents the capability of changing the beam separation in order to make different orders interfere properly. The interference patterns produced can be separately modulated through the operation of linear polarizer's placed on each interference replica. In order to present the capabilities of the system we will select four interferograms result of contiguous orders interference.

1. Introduction

In this work, we propose a simple optical system that allows the capture of *n*-interferograms with controllable relative phase shifts in a single capture. The optical arrangement presented is based on principles of polarization phase shifting techniques [1] and grating interferometry [2,3]. A common polarizing optical system uses linear polarizing filters and quarter-wave plates (QWP) to achieve modulation [1], one of the most relevant are the micropolarizers arrays [4] and others authors have proposed an improvements of them using harmonics rejections algorithms or the use of nine shifts [5]. These systems present the advantage of not requiring mechanical components such as piezo-electric mirror, or special diffractive elements to obtain a phase shift in the interferograms, hence the system is insensitive to external vibrations.

The proposed optical system presents mechanical stability against external vibrations, due to the two beams generated by a polarizing beam splitter (PBS) are common path. The two beams are redirected to a 4-*f* system. A diffraction grid collocated at Fourier plane produces replicas of the two beams, which interfere to generate *n*-interferograms. The phase shifts between the interferograms can be generated by polarization components. This system allows us to measure the phase profile with high accuracy. A difference with the systems presented by our groups in Ref. [2] and Ref. [5] is that we used a two-window arrangement with fixed separation, designed in accordance with the grating used and the matching condition $x_0 = \lambda f/d$, where x_0 is the beam separation, d the spatial period and λ the wavelength of the source. The optical set-up presented here generates two beams whose separation can be adjusted according to the characteristics of the components used, such as the grating or lens.

In order to reduce the use of more expensive components, like phase gratings used before, we are proposing the use of low cost amplitude gratings for the generation of replicas of the interfering beams. Too some considerations are proposed in this experiment.

2. Experimental setup

Fig. 1 shows the experimental setup used. When a quarter wave plate (Q) and a linear polarizing filter P_0 intercept a laser beam, it is generated linearly polarized light oriented at 45°. The light comes from a He–Ne laser operating at $\lambda = 632.8$ nm. Fig. 1(a) shows a polarizing beam splitter which divide the beam into two beams A and B with orthogonal linear polarizations. The spacing between the beams, x_0, it can be controlled by a displacement between the

---

* Corresponding author. Tel.: +55 294 9422796.
E-mail addresses: beleloort@gmail.com (B. Lopez-Ortiz), noel.toto@utec-tgo.edu.mx (N.-I. Toto-Arellano).

http://dx.doi.org/10.1016/j.ijleo.2014.07.131

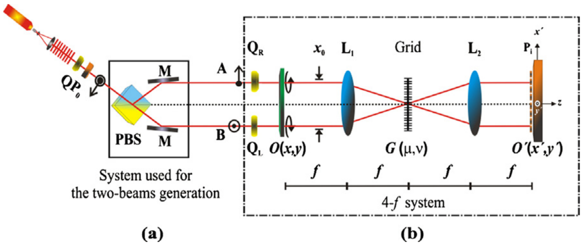

Fig. 1. Experimental setup. Q_i: quarter wave plate, P_i: polarizing filters. PBS: polarizing beam splitter; M: mirror. Beams: A, B. L_i: lens, $G(\mu,\nu)$: Grid. x_0: beam separation. $O(x,y)$: object plane. $O'(x',y')$: image plane.

mirrors M. Quarter wave plates QL (45) and QR (−45) are placed in each one of the beams respectively, to generate a right circular polarizations in A and left circular polarizations in B. This system is simpler than other arrangements previously presented such as Mach Zehnder interferometer [2] or a common path configuration [3] that have been used to generate a double window.

The system in Fig. 1(a) is coupled to a 4-*f* arrangement which has two similar achromatic lenses (focal length $f = 250$ mm) and a grid $G(\mu,\nu)$ placed at the system's pupil (spatial period $d = 0.01$ mm). In the image plane can be observed interference patterns which are obtained from the superposition of the replicas of windows A and B, centered in each diffraction order. The result is *n*-interference patterns.

The phase shifts can be operated independently by placing of linear polarizer over each interference pattern. Each polarizing filter is adjusted at a different angle ψ to obtain the desired phase shift. In the arrangement shown in Fig. 1, the Beam A is the reference beam whereas that the target object is placed intercepting the beam B.

3. Interferometry using an amplitude grid

In the one-dimensional case the amplitude transmission of an amplitude grating can be written as the periodic function [6]

$$G(\mu) = rect\left[\frac{\mu}{a_w}\right] \otimes \sum_{n=-N}^{\infty} \delta\left[\frac{\mu - nd}{a_w}\right] \tag{1}$$

with μ denoting the object space, $d = a_w + b_w$ being the grating period, a_w and b_w being the widths of the clear and dark bands respectively (in this case it is considered that the separation between dark and clear bands is the same), $\delta(\mu)$ denoting the Dirac delta function, and $\otimes$ indicating convolution. Thus, the Fourier transform of Eq. (1) with $N \to \infty$ is given by:

$$\begin{aligned}\tilde{G}(x) &= \frac{a_w}{d}\sin c(a_w x)\sum_{n=-\infty}^{\infty}\delta\left(x - \frac{n}{d}\right)\\ &= \frac{a_w}{d}\sum_{n=-\infty}^{\infty}\sin c\left(a_w\frac{n}{d}\right)\delta\left(x - \frac{n}{d}\right) = \sum_{n=-\infty}^{\infty} C_n \cdot \delta\left(x - \frac{n}{d}\right),\end{aligned} \tag{2}$$

where C_n results as the *n*-Fourier complex coefficient of $G(\mu)$. In general, a grid, placed on the Fourier plane, can be generated by the multiplication of two gratings placed with their axes orthogonally oriented:

$$G(\mu,\nu) = \left\{rect\left[\frac{\mu}{a_x}\right] \otimes \sum_{n=-N}^{N}\delta\left[\frac{\mu - nd}{a_x}\right]\right\}\left\{rect\left[\frac{\nu}{a_y}\right] \otimes \sum_{l=-L}^{L}\delta\left[\frac{\nu - nd}{a_y}\right]\right\}, \tag{3}$$

where N, L are the numbers of components of the grating, d is the same period along the directions "x" and "y", and a_x, a_y are the widths in clear strips along each one of both directions. Due to the properties of the Fourier transform, the corresponding spectrum is:

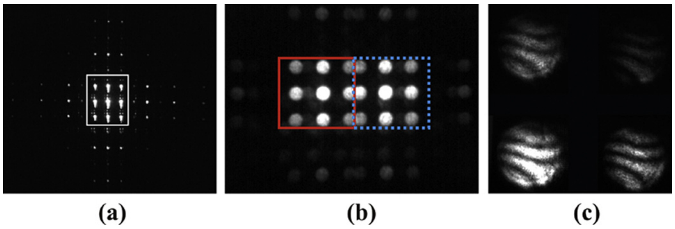

Fig. 2. (a) Diffraction orders generated by the grid. (b) Replicas of the two beams generated by the grating. (c) Interference patterns used to recover the optical phase.

$$\begin{aligned}\tilde{G}(x,y) = \tilde{G}(x)\cdot\tilde{G}(y) &= \frac{a_w^2}{d^2}\sum_{n=-N}^{N}\sin c\left(\frac{a_w}{d}\cdot x\right)\\ &\cdot\delta\left(x - \frac{n}{d}\right)\sum_{l=-L}^{L}\sin c\left(\frac{a_w}{d}y\right)\cdot\delta\left(y - \frac{l}{d}\right)\\ &= \sum_{n=-N}^{N} C_n \cdot \delta\left(x - \frac{n}{d}\right)\sum_{l=-L}^{L} C_l \cdot \delta\left(y - \frac{l}{d}\right).\end{aligned} \tag{4}$$

These coefficients C_n and C_l will modulate the intensity pattern obtained at the image plane [2,3].

3.1. Replicas of the interference patterns and phase shifts

The interference patterns are obtained of the interference between the replicas of beams A and B. Fig. 2 shows some representative results corresponding how the grid generates replicas of the beams A and B. Fig. 2(a) shows the diffraction pattern generated by a grid, it can be appreciated the changes in intensity and modulation in each replica, due to the properties of diffraction gratings which form the grid. Fig. 2(b) shows the replicas of the beam A (with right circular polarization) and the replicas of the beam B (with left circular polarization). As has already been mentioned, the separation of the beams can be adjusted to have interference between the orders $[(0,-1)(+1,0)]$ respectively. Interferograms with the same modulation and amplitude are obtained to the process of the retrieve of optical phase using the known four-step algorithm. Finally, Fig. 2(c) shows the resulting interference patterns.

4. Phase shifts generated by polarization

Taking into account that each beam has left and right circular polarization and the intensity is modulated by the Fourier coefficients C_n and C_l. After placing a linear polarizer at an angle ψ, the resulting interference pattern obtained is $I(x,y)$

$$I(x,y) = \left|A\cdot\sum_{n,l}^{\infty} C_{n.l} + B\cdot\sum_{n,l}^{\infty} C_{m+1,n}\cdot e^{i\phi\left[\left(x+\left(n+\frac{1}{2}\right)\cdot d,(y+l\cdot d)\right)\right]}\right|^2 \tag{5}$$

with A and B, the amplitudes of each beam, given by:

$$A = J_\psi \vec{J}_L, \quad B = J_\psi \vec{J}_R, \tag{6}$$

where the Jones vectors corresponding to left and right circular polarizations are defined as:

$$J_L = \begin{pmatrix}1\\ i\end{pmatrix} \quad J_R = \begin{pmatrix}1\\ -i\end{pmatrix} \tag{7}$$

and J_ψ is the corresponding matrix of a polarizer at an arbitrary angle ψ. We can show that Eq. (5), can be simplified to:

$$I(x,y) = (C_{n.l})^2 + (C_{n+1,l})^2 + 2\cdot C_{n,l}\cdot C_{n+1,l}\cdot\cos[2\cdot\psi + \phi(x,y)]. \tag{8}$$

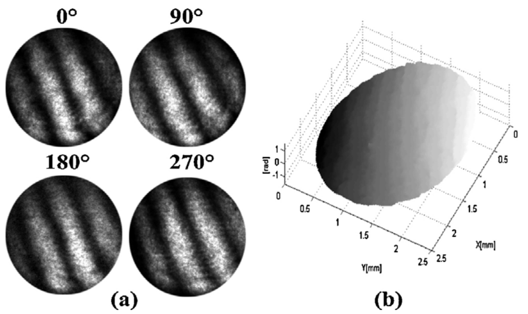

Fig. 3. Reference wavefront. (a) Interference patterns captured simultaneously with relative phase shifts of $\pi/2$. (b) 3D phase profile.

Considering that the amplitudes and modulation are comparable, Eq. (8) can be simplified as:

$$I_i(x, y) = 1 + \cos\left[2\cdot\psi_i - \phi(x, y)\right], \tag{9}$$

where $I_i(x,y)$ represents the intensity distribution with $i = 1,\ldots,4$ captured by the CCD camera in a single shot. The polarization filters angles are: $\psi_1 = 0^\circ$, $\psi_2 = 45^\circ$, $\psi_3 = 90^\circ$ and $\psi_4 = 135^\circ$, and each one of them represents phase shifts ξ of $0, \pi/2, \pi$ and $3\pi/2$ respectively.

To minimize errors in amplitude generated by the placement of polarizers at different angles [7,8], every interferogram used was subjected to a rescaling and normalization process, using digital image processing techniques [9,10]. This procedure generates patterns of equal intensities. The relative phase can be calculated as:

$$\tan\phi = \frac{I_2 - I_4}{I_1 - I_3} \tag{10}$$

The method used for unwrapping the phase data was a Quality-Guided Path Following method [10].

5. Experimental results

Experimental results were obtained with the optical system proposed. A monochromatic camera (CMOS) with 1280 × 1024 pixels was used in the capture of the images. Fig. 3(a) shows the interference patterns generated by the proposed optical system when illuminated with the reference wavefront. The phase obtained from the processing of the interferograms was used as a reference phase map, and subtracted from the phases obtained for the rest of the cases presented. The phase shown in Fig. 3(b) represents the phase of a wavefront with tilt.

Fig. 4 shows the results obtained for a sample of glass slide on which a phase step of a wide of 0.5 mm was manufactured. In the interference patterns retrieved, the ends of the striped groove on the glass slides can be clearly seen (see Fig. 4(a)). Fig. 4(b) shows the retrieved phase obtained for this sample.

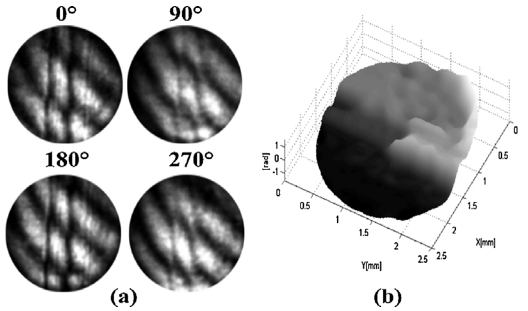

Fig. 4. Phase step marking on a slide. (a) Interference patterns captured simultaneously with relative phase shifts $\pi/2$. (b) 3D phase profile.

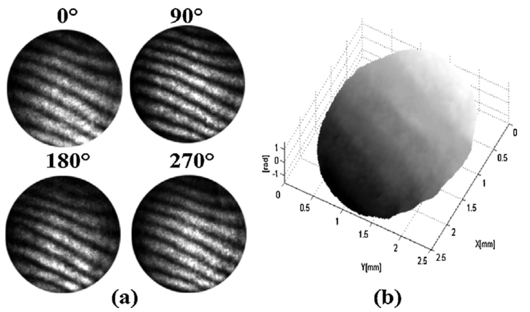

Fig. 5. Acetate plate subjected to tension. (a) Interference patterns captured simultaneously with relative phase shifts $\pi/2$. (b) 3D phase profile.

Fig. 5 shows the results obtained with an acetate plate. The object consisted of elastic surface of 2.5 cm × 2.5 cm, clamped rigidly at one end. The free end of the surface is clamped and get out uniformly. For the purpose of the presentation of data, the target object is subjected to only in-plane-*y* deformation.

This load produces in-plane and out-of-plane deformations, which can be detected by the kind object illumination. It can be seen that a change in the frequency of the fringes in relation to the reference interference pattern. The phase recovered through the methods given is shown in Fig. 5(b).

6. Conclusions

A polarizing phase shifting two-windows interferometer with grid has been described. The optical system permits to obtain the optical phase data of phase objects using four interferograms in single capture. The presented technique can be used in the measurement of dynamic phase objects. The combination of amplitude grids and conventional polarizing elements optimizes the interferometric system and simplifies other arrangements previously presented, where a Mach–Zehnder interferometer or a common path configuration have been used to generate a double window.

Acknowledgments

This research was partially supported by the Technological University of Tulancingo, according to the initiative for the creation of the First *Optics and Photonics Engineering* undergraduate program in Mexico. Authors thank M.A. Ruiz for his contribution in proofreading the manuscript, comments and references from anonymous referees are also acknowledged. Author N.-I. Toto-Arellano expresses sincere appreciation to Luisa, Miguel and Damian for the support provided. Author V.H. Flores Muñoz is grateful to CONACYT for the scholarship provided (Grant. 224506).

References

[1] R.M. Neal, J.C. Wyant, Polarization phase-shifting point-diffraction interferometer, Appl. Opt. 45 (2006) 3463–3476.
[2] N.I. Toto-Arellano, et al., Measurement of the dynamic phase profile of transparent fluids, Opt. Pura Apli. 46 (2013) 21–28.
[3] N.I. Toto-Arellano, D.I. Serrano-García, A. Martínez García, G. Rodríguez Zurita, A. Montes-Pérez, 4D profile of phase objects through the use of a simultaneous phase shifting quasi-common path interferometer, J. Opt. 13 (2011) 115502.
[4] J.C. Wyant, Dynamic interferometry, Opt. Photon. News 14 (2003) 36–41.
[5] G. Rodriguez-Zurita, N.I. Toto-Arellano, C. Meneses-Fabian, J.F. Vázquez-Castillo, One-shot phase-shifting interferometry: five, seven, and nine interferograms, Opt. Lett. 33 (23) (2008) 2788–2790.
[6] N.I. Toto-Arellano, A. Martinez-Garcia, G. Rodriguez-Zurita, J.A. Rayas-Alvarez, A. Montes-Perez, Slope measurement of a phase object using a polarizing

phase-shifting high-frequency Ronchi grating interferometer, Appl. Opt. 49 (2010) 6402–6410.

[7] A.-H. Phan, M.-I. Piao, J.-H. Park, N. Kim, Error analysis in parallel two-step phase-shifting method, Appl. Opt. 52 (2013) 2385–2393.

[8] N.-I. Toto-Arellano, V.H. Flores-Muñoz, B. Lopez-Ortiz, Dynamic phase imaging of microscopic measurements using parallel interferograms generated from a cyclic shear interferometer, Opt. Express 22 (2014) 20185–20192.

[9] D. Malacara, M. Servin, Z. Malacara, Phase Detection Algorithms in Interferogram Analysis for Optical Testing, Wiley, New York, 2005.

[10] C. Ghiglia, M.D. Pritt, Two-Dimensional Phase Unwrapping: Theory, Algorithms, and Software, John Wiley & Sons, New York, 1998.